J Fluoresc (2007) 17:43–48
DOI 10.1007/s10895-006-0145-1

ORIGINAL PAPER

Fluorescence Lifetime Correlation Spectroscopy

Peter Kapusta · Michael Wahl · Aleš Benda · Martin Hof · Jörg Enderlein

Received: 19 July 2006 / Accepted: 13 October 2006 / Published online: 17 November 2006

Abstract This article explains the basic principles of FLCS, a genuine fusion of Time-Correlated Single Photon Counting (TCSPC) and Fluorescence Correlation Spectroscopy (FCS), using common terms and minimum mathematics. The usefulness of the method is demonstrated on simple FCS experiments. The method makes possible to separate the autocorrelation function of individual components of a mixture of fluorophores, as well as purging the result from parasitic contributions like scattered light or detector afterpulsing.

Keywords FCS · TCSPC · Lifetime · Correlation · Multichannel detection · Scattering · Afterpulsing

Introduction

The combination of Time-Correlated Single Photon Counting (TCSPC) and Fluorescence Correlation Spectroscopy (FCS), called Fluorescence Lifetime Correlation Spectroscopy (FLCS), is a method that uses picosecond time-resolved detection for *separating* different FCS contributions. The emphasis is on the word *separating*. FLCS does not involve fitting of a multiple-parameter model to a complex autocorrelation function. Instead, a *separate* autocorrelation function is calculated for each fluorescence lifetime component, emitted for example by various species in the sample. The only assumption is that the various components have distinct and non-changing lifetime signatures. The core of the method is a statistical separation of different fluorescence contributions on a single photon level.

An essential requirement for FLCS is a sub-nanosecond pulsed excitation instead of continuous wave (CW) illumination. The second requirement is the ability to simultaneously measure the fluorescence photon arrival time on two different time scales: relative to the excitation pulse with picosecond resolution (TCSPC) and relative to the start of the experiment with nanosecond precision.

The experimental and analysis technique outlined is an important extension of standard FCS. The core idea appeared in 2001 [1] but received only a little attention until now, although recent publications [2, 3] present exciting new applications of this method.

The principle

FLCS is best understood in comparison with conventional FCS using CW excitation and single channel detection. The standard result of an FCS experiment is the autocorrelation function (ACF) of the fluorescence intensity fluctuations. This can be calculated by a hardware autocorrelator, but the recent state-of-the-art is to use more versatile software processing of recorded individual photon arrival times [9]. The core problem of FCS is that if the detected signal contains more than one component, the resulting ACF is a linear combination of the contributions from the different components. A trivial example is a sample with two kinds of diffusing

P. Kapusta (✉) · M. Wahl
PicoQuant GmbH,
Rudower Chaussee 29,
12489 Berlin, Germany
e-mail: photonics@picoquant.com

A. Benda · M. Hof
J. Heyrovský Institute of Physical Chemistry, Academy of Sciences of the Czech Republic,
Dolejškova 3,
18223 Prague, Czech Republic

J. Enderlein
IBI-1, Forschungszentrum Jülich in der Helmholtzgesellschaft,
52425 Jülich, Germany

fluorophores, both contributing to the detected intensity fluctuations. Taking into account the ubiquitous triplet dynamics, scattered excitation light, impurity fluorescence etc., the analysis of the resulting ACF becomes challenging due to the number and mutual influence of adjustable parameters in the model equation used for fitting. *Resolving* an ACF is difficult [4].

In FLCS data acquisition, the excitation is pulsed and two independent timings are performed for every detected photon event. The *macroscopic* arrival measured with respect to the start of the experiment on a continuous time axis contains information related to e.g. translational motion, triplet lifetime etc., and is used just like in conventional FCS. The delay time measured relative to the excitation pulses contains information about the fluorescence decay on a nanosecond timescale. It is the simultaneous availability of these two independent timings that makes possible to calculate *separate* ACF for the selected lifetime component.

Let us start with a simple example. Consider a sample with two fluorescent components, A and B, which have different fluorescence decay kinetics. Let us assume that, say, 60% of all photons captured during an FLCS experiment were emitted by compound A and the rest by B. After each excitation pulse, the photon detection probability decays on a nanosecond time scale, as shown in Fig. 1. In TCSPC, this time scale

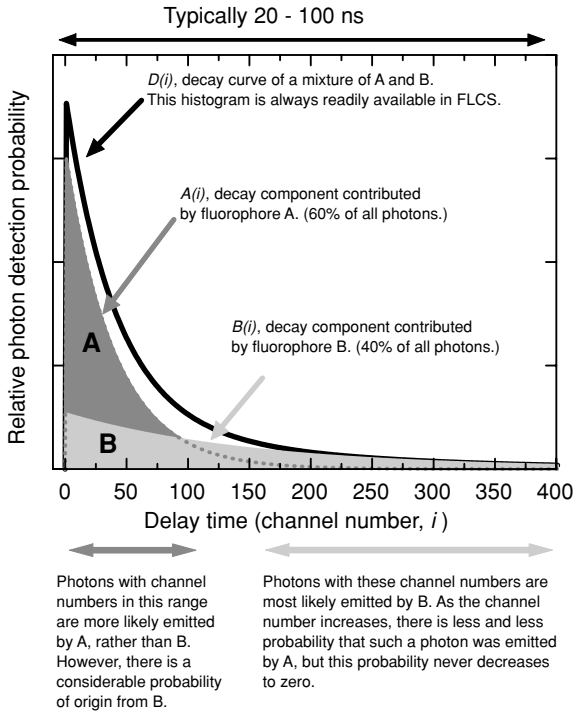

Fig. 1 A hypothetical TCSPC histogram of a two-component mixture, $D(i)$, and its component decays, $A(i)$ and $B(i)$. The histogram $D(i)$ is readily available after any FLCS measurement, while the shape of $A(i)$ and $B(i)$ can be obtained from independent TCSPC measurements or from the analysis (e.g. fitting) of $D(i)$

is binned into N channels indexed by their number i, so that $i = 1, \ldots, N$. Typically, N is on the order of 100–1000. By histogramming the frequency of various channel numbers encountered and neglecting their macroscopic arrival times one gets the conventional TCSPC decay curve $D(i)$.

The measured decay histogram is a superposition of contributions from A and B, but if the decay characteristics of both components are known *a priori*, the relative contributions of each component can be extracted by deconvolving the measured histogram. FLCS uses this ability to separate contributions based on their lifetime signature, a feat impossible when using CW excitation.

Next, we will explain how to use the TCSPC information for calculating lifetime-specific ACFs. Let us assume that the TCSPC histograms of the pure components are known (e.g. from *a priori* measurements on pure samples, or from decay curve analysis) and are denoted by $A(i)$ and $B(i)$. Let us normalize $A(i)$ and $B(i)$ as $a(i) = A(i)/\Sigma A(i)$, $b(i) = B(i)/\Sigma B(i)$, so that $\Sigma a(i) = \Sigma b(i) = 1$. We will refer to these normalized curves as *decay patterns*. The experimentally obtained decay curve of a mixture, $D(i)$, can then be expressed as the linear combination

$$D(i) = w_a \cdot a(i) + w_b \cdot b(i) \tag{1}$$

where w_a and w_b are the numbers of photons stemming from compound A and B, respectively. Let us now define two *filter functions*, $f_a(i)$ and $f_b(i)$, with the following property:

$$\langle \Sigma f_a(i) \cdot D(i) \rangle = w_a \quad \langle \Sigma f_b(i) \cdot D(i) \rangle = w_b \tag{2}$$

The brackets $\langle \cdots \rangle$ denote averaging over an infinite number of measurements. In addition, let $f_a(i)$ and $f_b(i)$ minimize the relative errors expressed as

$$\langle (\Sigma f_a(i) \cdot D(i) - w_a)^2 \rangle \quad \langle (\Sigma f_b(i) \cdot D(i) - w_b)^2 \rangle \tag{3}$$

As can be seen from the above expressions, the $f_a(i)$ and $f_b(i)$ act indeed like statistical filters or weighting functions applied to the total decay histogram, $D(i)$. They recover the number of photons contributed by each decay component.

Such filters can be numerically calculated from $D(i)$ and from the decay patterns $a(i)$ and $b(i)$ with simple matrix calculations [1]. To simplify the notation we introduce the abbreviations $\boldsymbol{a} = a(i)$, $\boldsymbol{b} = b(i)$, $\boldsymbol{f_a} = f_a(i)$ and $\boldsymbol{f_b} = f_b(i)$. The decay patterns and filter functions are thus understood to be row vectors of length N. It was shown in previous work [1, 3, 5] that, if the photon counting data obey a Poissonian statistics (which is usually the case for photon counting data), the two filter functions which fulfill the requirements of Eqs. (2) and (3) can be calculated as:

$$\begin{vmatrix} \boldsymbol{f_a} \\ \boldsymbol{f_b} \end{vmatrix} = \left(\begin{vmatrix} \boldsymbol{a} \\ \boldsymbol{b} \end{vmatrix} \cdot \boldsymbol{D} \cdot \begin{vmatrix} \boldsymbol{a} \\ \boldsymbol{b} \end{vmatrix}^T \right)^{-1} \cdot \begin{vmatrix} \boldsymbol{a} \\ \boldsymbol{b} \end{vmatrix} \cdot \boldsymbol{D} \tag{4}$$

where the dot $\cdot$, superscript T and -1 denote matrix multiplication, transposition and inversion, respectively. $\boldsymbol{D}$ is a diagonal $N \times N$ matrix constructed from the reciprocal values of counts in the histogram $D(i)$.

$$\boldsymbol{D} = \begin{vmatrix} \frac{1}{D(1)} & 0 & 0 & \cdots & 0 \\ 0 & \frac{1}{D(2)} & 0 & \cdots & 0 \\ \vdots & \vdots & \vdots & \vdots & \vdots \\ 0 & 0 & \cdots & 0 & \frac{1}{D(N)} \end{vmatrix} \tag{5}$$

All involved calculations are standard matrix manipulations, supported by many mathematical software packages and even spreadsheet applications.

Note that in Eq. (4) the two filters are calculated together, involving only one matrix inversion. Ensuring the orthonormality of decay patterns with the resulting filter functions, i.e. $\boldsymbol{f_a} \cdot \boldsymbol{a} = \boldsymbol{f_b} \cdot \boldsymbol{b} = 1$ and $\boldsymbol{f_a} \cdot \boldsymbol{b} = \boldsymbol{f_b} \cdot \boldsymbol{a} = 0$, is essential in order to fulfill the simultaneous requirements of Eqs. (2) and (3). In contrast, if $\boldsymbol{f_a}$ and $\boldsymbol{f_b}$ would be calculated separately as $\boldsymbol{f_a} = (\boldsymbol{a} \cdot \boldsymbol{D} \cdot \boldsymbol{a}^{\mathrm{T}})^{-1} \cdot \boldsymbol{a} \cdot \boldsymbol{D}$ and $\boldsymbol{f_b} = (\boldsymbol{b} \cdot \boldsymbol{D} \cdot \boldsymbol{b}^{\mathrm{T}})^{-1} \cdot \boldsymbol{b} \cdot \boldsymbol{D}$, they would be useless. Equation (4) is a special case of a more general formula for an arbitrary number x of decay components:

$$\begin{vmatrix} \boldsymbol{f_a} \\ \boldsymbol{f_b} \\ \vdots \\ \boldsymbol{f_x} \end{vmatrix} = \left(\begin{vmatrix} \boldsymbol{a} \\ \boldsymbol{b} \\ \vdots \\ \boldsymbol{x} \end{vmatrix} \cdot \boldsymbol{D} \cdot \begin{vmatrix} \boldsymbol{a} \\ \boldsymbol{b} \\ \vdots \\ \boldsymbol{x} \end{vmatrix}^{T} \right)^{-1} \cdot \begin{vmatrix} \boldsymbol{a} \\ \boldsymbol{b} \\ \vdots \\ \boldsymbol{x} \end{vmatrix} \cdot \boldsymbol{D} \tag{6}$$

It is valuable to have a look at the shape of $f_a(i)$ and $f_b(i)$ calculated for our hypothetical example. The filters corresponding to the decays depicted in Fig. 1 are plotted in Fig. 2.

The key point is that using $f_a(i)$ and $f_b(i)$ makes possible to statistically separate the contributions of A and B, photon by photon. In other words, the sign and magnitude of a single photon contribution to the autocorrelation can be determined from the photon's channel number using the corresponding filter function.

When correlating the photon records by a conventional FCS approach, every photon contributes equally and the calculation involves only zeros and ones. In FLCS, the filter value corresponding to the photon's channel number is used instead. The numbers entering the ACF calculation are therefore not integers, their absolute value can exceed one, and their sign can even be negative. However note that the sum

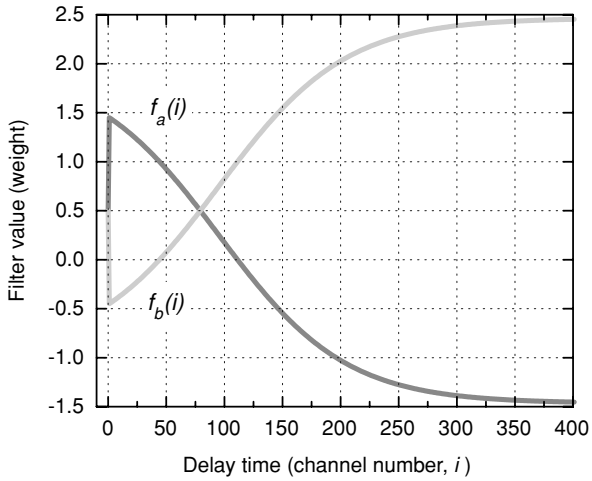

Fig. 2 Filter functions ('weights') calculated from $D(i)$, $A(i)$ and $B(i)$ according to Eq. (4)

of the filter values corresponding to a given channel number is always one.

The statistical interpretation of Fig. 2 is as follows: Due to the high fractional intensity of A at the beginning of the decay, photons with small channel numbers contribute to the ACF of compound A with an increased weight (> 1). Since every photon carries a unit intensity, they must simultaneously contribute with negative weight to the ACF of B. The vast majority of detected photons have small channel numbers (see Fig. 1) and it may be puzzling how one can get a physically meaningful ACF of compound B. The initial bias towards compound A will be compensated by the remaining photons. For example those with $i > 110$ contribute with an increased weight to the ACF of compound B and with negative weight to the ACF of A. Because such photons are rare, the absolute values of $f_a(i)$ and $f_b(i)$ for these channels are accordingly higher.

In brief, owing to the orthonormality of the filter functions with respect to the decay patterns, applying the $f_a(i)$ filter during software correlation of *all* photons one obtains the separate ACF of compound A. The same holds for $f_b(i)$ and compound B. Because the weighting is statistical in principle, a sufficient (time-)averaging is necessary: the more photons one has, the better is the accuracy of the resulting ACF. Of course, this also depends on how large the difference between decay patterns is. Typical FCS measurements collect more than 10^6 photons and the separation works reliably, as demonstrated in papers [1–3] and also in the following sections.

Instrumentation

The measurements reported below were performed with a MicroTime 200 confocal time-resolved fluorescence microscope [6] equipped with LDH635 pulsed red diode laser

driven by PDL800-B driver. The timing electronics of this system is based on the TimeHarp 200 PC board operated in a so-called Time-Tagged Time-Resolved (TTTR) mode [7, 8]. (All mentioned devices: PicoQuant GmbH, Berlin, Germany). Experimental data were processed and the calculations were performed on a PC using MatLab (MathWorks Inc., Natick, USA) and the fast correlation algorithm published in [9].

Application example 1: Suppression of scattered light and various parasitic contributions

At very low concentrations as encountered in FCS, a considerable portion of the detected intensity may come from Rayleigh and Raman scattered excitation light. In this example the sample was a 10 pM solution of Atto655 in ethylene glycol. Analysis of the TCSPC histogram (Fig. 3a) reveals that only approximately 60% of the photons are emitted by Atto655 molecules. The decay pattern of "pure" Atto655 was obtained in a separate measurement of a 1 nM solution, where the fraction of parasitic contributions can be neglected. First, the histogram of parasitic contributions was determined by subtraction of the appropriately scaled Atto655 pattern from $D(i)$ (Fig. 3a). As can be seen in Fig. 3c, filtering out the scattered photons has a striking impact on the resulting ACF.

Theoretically, the reciprocal value of the ACF in the limit of zero lag time gives the average particle number within the detection volume, that is, the concentration. The black curve was calculated without filtering and represents the standard FCS result. FLCS yields the correct particle number consistent with the sample concentration and detection volume size. The amplitude of non-filtered ACF is much smaller, because the influence of scattered photons is strongly nonlinear. Their contribution to the total detected intensity is only about 40%, but the apparent particle number is increased by a factor of more than 3. Standard FCS clearly fails to recover the correct sample concentration.

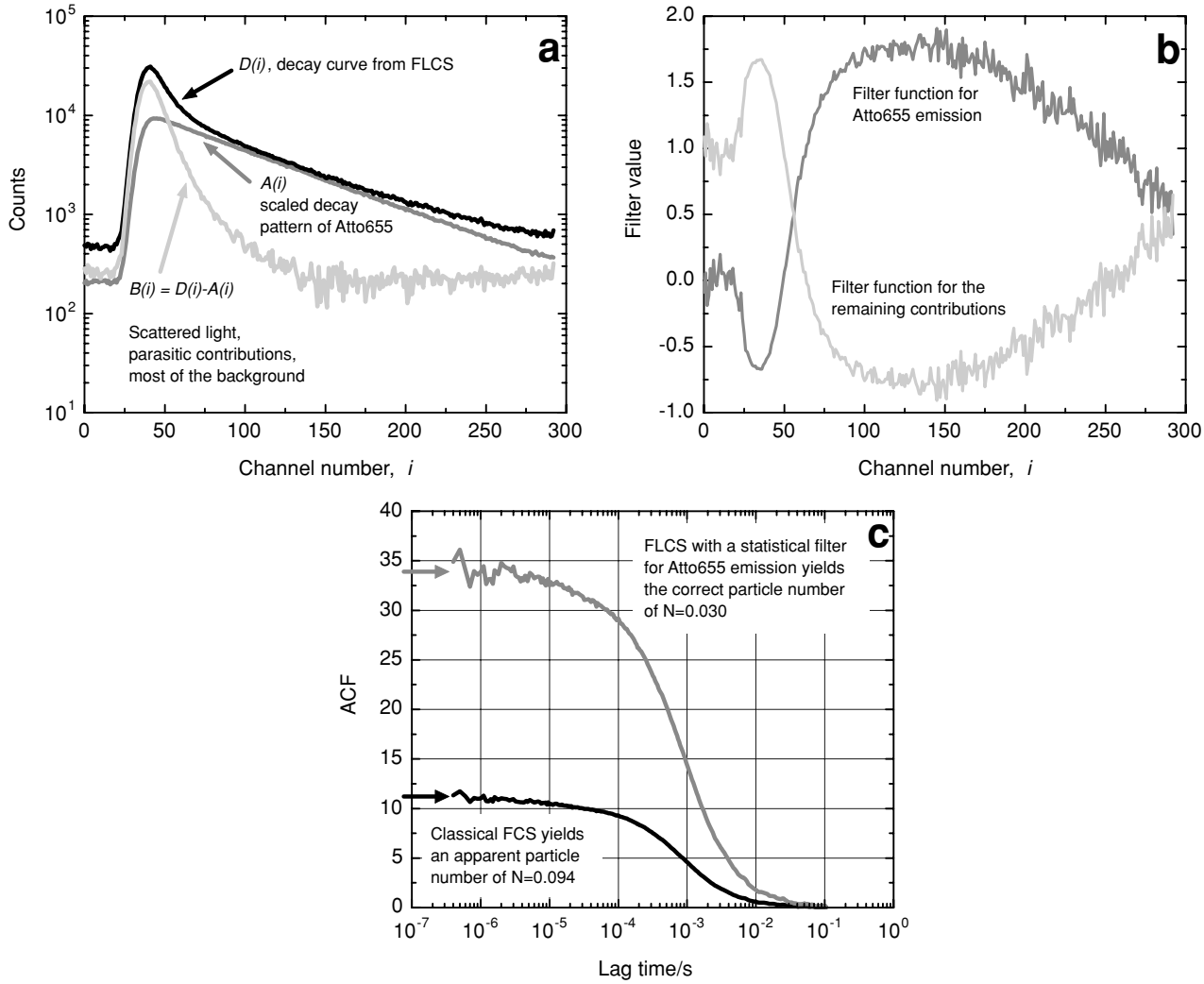

Fig. 3 Suppression of the scattered light contribution. (a) TCSPC histograms, (b) Calculated filter functions, (c) Comparison of FCS and FLCS results

In the above example, the only additional information gathered from an independent measurement was the undistorted decay pattern of Atto655. FLCS was used to obtain the ACF of the intensity contribution matching that decay pattern. The other filter, $f_b(i)$ is useless in a sense that using it one obtains only the ACF of scattering and dark counts, that is, a very noisy fast decaying ACF. However, for a mixture of fluorophores it is possible to obtain two decay patterns, so that both filters are useful. The ability of FLCS to separate the ACFs of two components (for example for simultaneous measurement of concentrations) was demonstrated in references [1] and [2]. A logical step further is cross-correlation analysis as described in [2].

Application example 2: Suppression of detector afterpulsing

Detector afterpulsing is a very common and often overlooked instrumental artifact that leads to a distortion of the ACF at short lag times, typically on a microsecond time scale. The resulting initial decay of an ACF can be easily misinterpreted as a triplet contribution. The suppression by means of FLCS is based on the fact that, at high excitation repetition rates, the spurious afterpulsing events are evenly distributed over the TCSPC histogram, appearing as a constant offset [3]. This very simple temporal behavior makes it easy to obtain the two patterns (Fig. 4a) and the corresponding statistical filters (Fig. 4b). Here the sample was a 100 pM water solution of Atto655 and the laser pulse repetition rate was 80 MHz. Of course, only the filter corresponding to the "pure" decay is suitable for correlation analysis.

The resulting ACF obtained with afterpulsing suppression by means of FLCS is shown in Fig. 4c. As can be seen, any fast decay on the microsecond time scale is eliminated when using FLCS, reflecting the fact the Atto655 does not have any discernible triplet state dynamics (Fig. 4d).

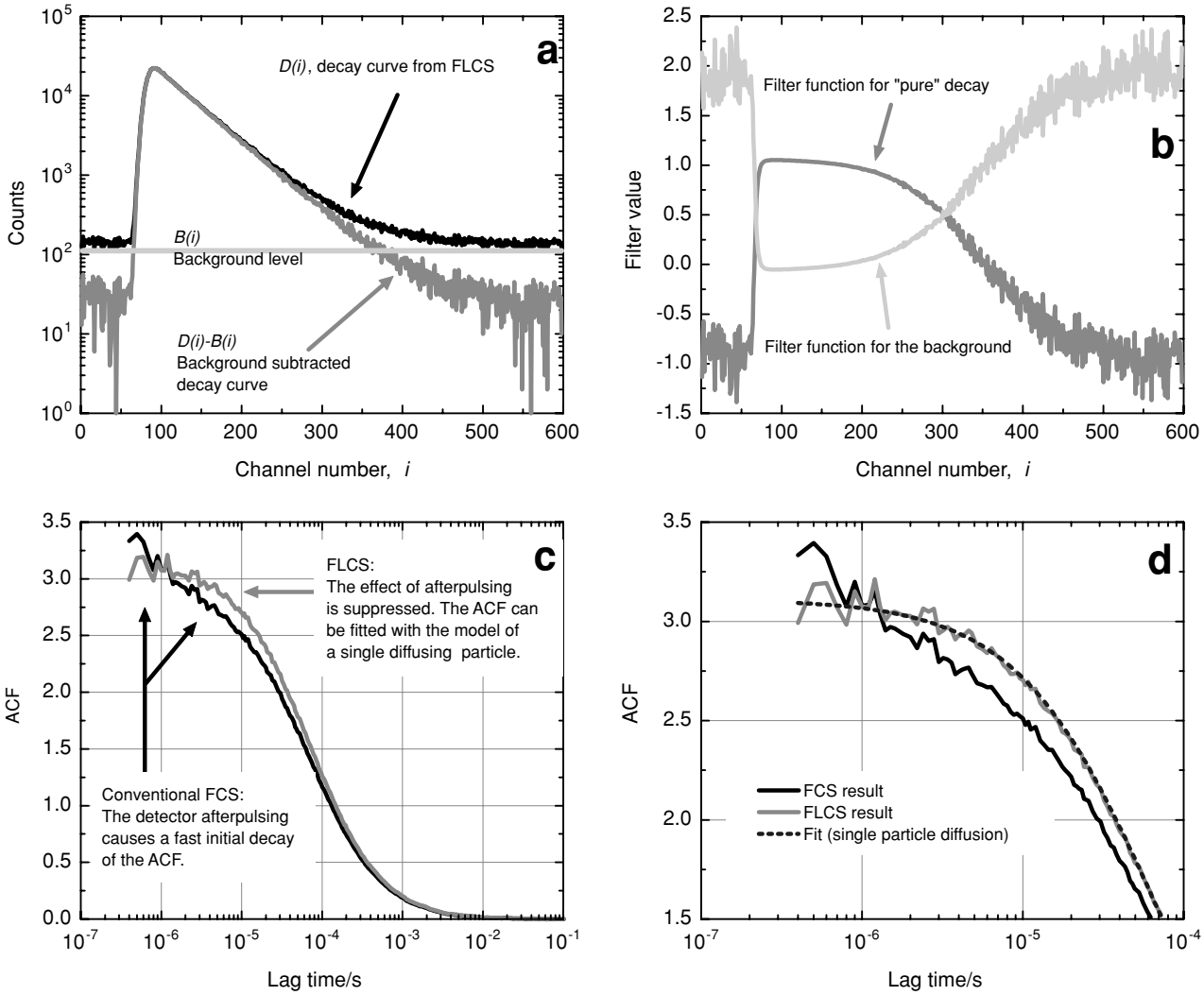

Fig. 4 Suppression of the effect of detector afterpulsing. (a) TCSPC histograms, (b) Calculated filter functions, (c) Comparison of FCS and FLCS results, (d) Detailed comparison of the ACFs at short lag times showing the agreement of the single particle diffusion model with the FLCS result

Conclusions and outlook

It was demonstrated that FLCS is an elegant extension of conventional FCS. The method can be regarded as an advanced form of time-gated FCS [10]. However, FLCS goes far beyond that, because it uses all the detected photons and separates the ACFs of different signal components quantitatively. Furthermore, the method represents a versatile quasi-multichannel detection scheme. In this sense, FLCS is a lifetime analogy of a multicolor FCS measurement, with several advantages.

Owing to the separation principle based on TCSPC decay behavior, distinct ACFs of two emitters can be obtained even if they have completely overlapping fluorescence spectra. For example, an ensemble of identical fluorophores localized in two different environments can display a double exponential decay. If a single lifetime can be associated with a certain environment, it is possible to quantitatively separate the two ACFs, or to cross-correlate the two lifetime components [11].

Even more contributions can be resolved provided that their decay patterns are sufficiently different. Looking at a real TCSPC histogram, the flat decay background and the sharp scattered light contribution are easily recognized. This makes an automatic suppression of these artifacts feasible, provided that there are no unresolved fast or exceedingly slow fluorescence decay components. In general, the functional form of the decay (single or multiple exponential, non-exponential) is irrelevant. Similarly, no assumptions are made on the form of the resulting ACFs. One can continue the analysis with the usual fitting of standard FCS models.

Unlike conventional FCS, concentrations of two compounds with very similar or even equal diffusion times can be monitored simultaneously. Once the intensity contributions are separated, cross-correlation is also straightforward [1, 2]. Note that the photon signal containing these contributions is recorded by a single detector. Hence the separately calculated ACFs correspond to the same detection volume, which can be interpreted as two (or more) perfectly overlapping excitation/detection volumes. This is very difficult to achieve in multicolor FCS experiments.

Finally, FLCS is easy to implement. It is not necessary to change the optical hardware of a standard FCS setup, because it contains almost all the required components. Affordable diode lasers are well suited for pulsed excitation. Of course, other excitation system generating picosecond pulses, based e.g. on a mode-locked laser, can be used as well. There are also several commercially available solutions for the second key component, the simultaneous measurement of the photon arrival time on two different time scales.

Acknowledgment A.B. and M.H. acknowledge financial support by the Ministry of Education and Sport of the Czech Republic via grant LC06063.

References

1. Böhmer M, Wahl M, Rahn H-J, Erdmann R, Enderlein J (2002) Time-resolved fluorescence correlation spectroscopy. Chem Phys Lett 353(5–6):439–445
2. Benda A, Hof M, Wahl M, Patting M, Erdmann R, Kapusta P (2005) TCSPC upgrade of a confocal FCS microscope. Rev Sci Instrum 76(3):033106
3. Enderlein J, Gregor I,(2005) Using fluorescence lifetime for discriminating detector afterpulsing in fluorescence-correlation spectroscopy. Rev Sci Instrum 76(3):033102
4. Meseth U, Wohland Th, Rigler R, Vogel H (1999), Resolution of fluorescence correlation measurements. Biophys J 76(3):1619–1631
5. Enderlein J, Erdmann R (1997) Fast fitting of multi-exponential decay curves. Opt Commun 134(1–6):371–378
6. Wahl M, Koberling F, Patting M, Rahn H-J, Erdmann R (2004) Time-resolved confocal fluorescence imaging and spectroscopy system with single molecule sensitivity and sub-micrometer resolution. Curr Pharm Biotechnol 5(3):299–308
7. Böhmer M, Enderlein J (2003) Fluorescence spectroscopy of single molecules under ambient conditions: Methodology and technology. Chem Phys Chem 4(8):792-808
8. Böhmer M, Pampaloni F, Wahl M, Rahn H-J, Erdmann R, Enderlein J (2001) Time-resolved confocal scanning device for ultrasensitive fluorescence detection. Rev Sci Instrum 72(11):4145–4152
9. Wahl M, Gregor I, Patting M, Enderlein J (2003), Fast calculation of fluorescence correlation data with asynchronous time-correlated single-photon counting. Opt Expr 11(26):3583–3591
10. Lamb DC, Schenk A, Röcker C, Scalfi-Happ C, Nienhaus GU (2000) Sensitivity enhancement in fluorescence correlation spectroscopy of multiple species using time-gated detection. Biophys J 79(2):1129–1138
11. Benda A, Fagulova V, Deyneka A, Enderlein J, Hof M (2006) Fluorescence lifetime correlation spectroscopy combined with lifetime tuning: New perspectives in supported phospholipid bilayer research. Langmuir 22(23):9580–9585